

Two-way Load Flow Analysis using Newton-Raphson and Neural Network Methods

Aya Al Shaltouni¹ and Abdulla Ismail²

¹MS of Electrical Engineering Student, Department of Electrical Engineering, Rochester Institute of Technology, Dubai, United Arab Emirates

²Professor, Department of Electrical Engineering, Rochester Institute of Technology, Dubai, United Arab Emirates

Abstract - This research presents a study of the optimal power flow for networked microgrids with multiple renewable energy sources (PV panels and wind turbines), storage systems, generators, and load. The OPF problem is performed using a conventional method and an Artificial Intelligence method. In this research, we investigated the performance of MGs system with renewable energy integration with focus on power flow studies. The calculation of the power flow is based on the well-known Newton-Raphson method and Neural Network method. The power flow calculation aims to evaluate the grid performance parameters such as voltage bus magnitude, angle, real and reactive power flow in the system transmission lines under given load conditions. The standard test system used was a benchmark test system for Networked MGs with four MGs and 40 buses. The data for the entire system has been chosen as per the IEEE Standard 1547-2018. The results showed minimum losses and higher efficiency when performing OPF using NN than the Newton-Raphson method. The efficiency of the power system for the networked MG is 99.3% using Neural Network and 97% using the Newton-Raphson method. The Neural Network method, which mimics how the human brain works based on AI technologies, gave the best results and better efficiency in both cases (Battery as Load/Battery as Source) than the conventional method.

Keywords: Optimal Power Flow, Microgrid, Newton-Raphson, Neural Network.

1. Introduction

The electric energy network is a complex and interconnected system commonly known as the grid. Growing electricity demand requires more sustainable and renewable energy sources. Nowadays, a massive transformation of the current electric energy system is observed. For instance, the energy flow becomes bidirectional due to the Distributed Generations (DG) plants where the energy is transferred between several nodes of the power grid/Microgrid, according to the changing demands [1].

A microgrid is a more intelligent and efficient mini-version of the electric grid. The electric grid is made up of interconnected sub-systems, namely generation, transmission, and distribution. On the other hand, the microgrid is a decentralized group of electricity sources and loads that are synchronized with the electrical grid but can be disconnected and operate autonomously in "Island Mode." It can serve a small localized area to keep the power flowing when the electrical grid is down, protect the microgrid from power outages by relying only on their own, serve the larger grid, and provide clean and green energy since they are fueled mainly by renewable energy sources (RES) [2].

Such a new scenario requires new systems that can allow the power grid to be smart by managing the bi-directional energy flow. Figure 1.1 shows the current plan where different distributed generation plants supply the energy to customers and the surplus power is injected back to the grid [1]. In addition, the improvements in storage technologies allow more flexible operation and reliable management of energy. Therefore, RES associated with storage units is considered as actively distributed generators, which is one of the essential elements of the "Smart Grid" concept [3].

Bulk power generators are complicatedly connected to the transmission system, whereas the simple design of distribution networks allow many customers to easily connect to them and be the prosumers. The Generating Companies (GenCos) seek to maximize the utilization of the existing generation resources by using the appropriate load distribution. However, the Transmission Companies (TransCo) tend to keep standard operating conditions in terms of low transmission line congestion, high value of minimum bus voltage, and low level of transmission loss [4]. Loss reduction can be achieved through the appropriate control of Distributed Generation (DG) resources in the distribution systems, or more generally, through the management of dispatchable resources (DG, load, storage), which can be effectively assessed using Optimal Power Flow problem.

1.1. Objective and Methodology

The employment of the OPF in smart grids is regarded as a new development in power system studies. Therefore, this work aims to study the optimal power flow problem in microgrid by determining the best way to optimize the flow of power using the Newton-Raphson approach and the Neural-Network approach. The optimization of the power flow using the Newton Raphson method and Neural-Network method will be performed using simulation. In addition, the impacts of the distributed generations, renewable energy sources, storage systems, and EV Charging stations are investigated.

1.2. Work Organization

Section II gives an overview of previous publications covering OPF. Section III gives an overview of the Optimal Power Flow. Section IV highlights the study of OPF using Newton-Raphson method. In Section V, the OPF Study using the Neural-Network is analyzed. Discussions and conclusions are drawn in Section VI and VII respectively.



Fig - 1.1 Current Scenario of the power grid.

2. Literature Review

Lin and shen [5] showed that utilizing renewable energy sources to reduce carbon emission and minimizing the fuel cost for energy saving in the OPF problem will reduce the global warming effect from the power generation sector. In this paper, a DPOPF (distributed and parallel OPF) algorithm for the smart grid transmission system with renewable energy sources was proposed to account for the fast variation of the power generated by renewable energy sources. The proposed DPOPF algorithm combines the recursive quadratic programming method, and the Lagrange projected gradient method. The proposed algorithm can achieve the complete decomposition and be implemented in the smart grid transmission system to make distributed and parallel computation possible. results confirm that the computing speed of the proposed DPOPF algorithm is fast enough to

cope with the fast variations of the power generated by renewable energy sources. A PSO (Particle Swarm Optimization) was presented in [6] to find the most optimal locations and sizes of DGs, with the objective function to minimize the system's total cost, real power loss, and the number of the installed DGs. Firstly, a radial distribution power flow (PF) algorithm is executed to find the global optimal solution. Then, with respect to voltage profile, THD and loss reduction and by using the sensitivity analysis, PSO is used to calculate the objective function and to verify bus voltage limits. To include the presence of harmonics, PSO was integrated with a harmonic power flow algorithm (HPF). The proposed (PSO-HPF) based approach was tested on an IEEE 15-bus radial distribution system. According to the authors, these scenarios yield efficiency in improvement of voltage profile and reduction of THD and power losses; it also permits an increase in power transfer capacity and maximum loading. According to Pazheri et al. [7], an economic/environmental dispatching (EED) problem formulation was presented for a hybrid system that comprises thermal units, the solar, wind, and storage unit. The study was simulated using MATLAB/Simulink. A consistent optimum EED was obtained by extracting maximum renewable energy during their availability and using them for both available and unavailable periods with the aid of their storages. In [8], Atwa et al. proposed a probabilistic planning technique to allocate various DG types (wind, solar, biomass) in the distribution system with an Objective Function to minimize the energy loss. The results reveal that regardless of the combination of the renewable resources used to calculate the optimal fuel mix, there is a significant reduction in the annual energy loss. An optimal control model of a heat pump water heater (HPWH) supplied by a wind-generator-PV-grid system was presented in [9] with an OF is to minimize the overall energy cost. This problem was solved using a mixed integer linear program. The results show a 70.7% cost reduction upon implementation of this intervention. Sanseverino et al. [10] showed an execution monitoring and re-planning approach to solve the optimal generation dispatch problem in smart grids with OF to minimize the carbon emissions, production costs and improve the quality. The replanning module is based on a heuristic multi-objective optimizer able to efficiently incorporate constraints. The obtained results were encouraging and suggest to incorporate into the Microgrids software technology approaches for managing uncertainties. A smart energy management system (SEMS) was presented in [11] to optimally organize the power production of DG sources and energy storage systems and minimize the microgrid operational costs. The results show that the forecasting model is able to predict hourly

power generation according to the weather forecasting inputs.

Similarly, an optimal energy management system of storage devices in grid-connected microgrids was presented in [12], where the stored energy is controlled to balance the loads and renewable sources and minimize the total cost of energy at the PCC (Point of Common Coupling). Bracale et al. [13] presented an optimal control approach for a DC microgrid that included dispatchable (micro-turbine) and non-dispatchable (PV generator) units, storage system, and controllable/non-controllable loads. It was designed to achieve a minimum daily total energy cost and it shows that the power provided by the dispatchable unit and the storage system allowed the minimization of the daily costs of energy. A novel OPF algorithm for islanded microgrid was presented in [14], where it provides minimum losses and a stable operating point with relevant droop parameters used to regulate the primary voltage and frequency. Shen et al. [15] presented an energy management scheme containing battery storage, diesel generators, PV, and wind. As a result, the proposed energy management system is effective in engineering practice and beneficial for both the microgrid and the customers. Hassanzadehfard et al. [16] employed battery banks as long-term storage and ultra-capacitors as short-term storage to control the frequency in a microgrid. The simulation results showed that considering interruptible loads for the microgrid results in cost reduction for the microgrid.

The development of EVs technology has a significant impact on microgrid operations. Yu et al. in [17] analyzed a model to find the effect of EV technology on-demand response mobility. Numerical results show that EVs mobility of symmetrical EV fleet is able to achieve synchronous stability of network and balance the power demand among different districts. Moreover, Laureri et al. [18] presented an optimization technique to integrate the EVs into the smart grids. The results prove that the integration of electric vehicles in the smart grids can help in sustaining the grid processes when parked and so playing in costs minimization. Paterakis et al. [19] developed an optimization technique to minimize the energy procurement costs of a smart household. Coordination strategy was proposed in order to satisfy the transformer capacity limits while promoting its economically fair usage by the households. Lin et al. [20] utilized an active power limitation strategy to reduce PV power injection during peak solar irradiation to avoid deviations in voltage. The results show that the control for PV power rejection increases the installation capacity of a PV system to make full use of solar energy resources and

to maximize the net present value of a PV system investment. Moreover, a study was conducted in [21] to find the optimal design of a PV/Battery hybrid system regarding PV modules' numbers, the PV module's tilt, batteries numbers, and capacities. Results show that the choice of installation place and of the system type can significantly affect the optimization results significantly. In particular, the optimum PV module tilt angle value changes according to electrical energy demand of the domestic utility. In [22], an optimization of the power flow of the PV system connected to the grid was presented. It was performed by calculating the root of the active and reactive power equation using Newton's Raphson method. Simulation results have shown the maximum value of the active power system at 1000 W/m² irradiation was 408 W, as the reactive power is needed only 11.82 Var. In [23], an application for optimization of the energy flows in smart power systems consisting of electric vehicles (EV), distributed energy sources (DER), flexible loads, and bidirectional storage is proposed, as well as an optimization model for energy distribution between electric vehicles, electric storage devices, and photovoltaic generators. A nonlinear optimization problem with linear constraints for optimizing the power flows in the system is defined and solved. A multi-objective problem is determined to satisfy PV production criteria and maximize the power flow to the EVs. An algorithm for finding the optimal solution to the multi-objective optimization problem is also proposed. The approach is beneficial for energy flow control and analysis of DER behavior. The algorithm proposed for solving the multi-objective problem is applicable when storage and PV generation units are used in the DER system.

Rigo-Mariani et al. [3] investigated different procedures for the optimal power dispatching of a grid-connected prosumer with energy storage consisting of a high-speed flywheel. According to the paper, optimal off-line scheduling for the day ahead aims to minimize the cost with regard to the daily energy rates and consider the forecasts for both consumption and production. That dispatching is performed using global optimization procedures based on a trust-region method or a niching genetic algorithm. Another approach developed by the authors in [3] is using step-by-step optimization and exploiting an original self-adaptive dynamic programming strategy. Kim and Lavrova [24] used an advanced optimization method to present optimal power flow and energy-sharing among smart buildings. The authors claimed that this method could improve the smart grid's optimal power flow and energy-sharing stability among smart buildings and enhance energy dissipation balance to reach stability among many smart buildings in the smart

grid.

Ke et al. [25] presented a new probabilistic OPF (POPF) model with chance constraints that reflect the uncertainties of wind power generation (WPG). The results show the satisfactory accuracy of the PLF (Probabilistic Load Flow) method, and the effectiveness of the proposed P-OPF model. In [26], a probabilistic AC OPF (POPF) was presented, considering the load variation, stochastic wind behavior, and variable line's thermal rating. It was observed that a reduction on the mean cost and also on the probability of reaching higher generation costs was obtained when dynamic limits were used. An optimization system to calculate the optimal operation of a system comprising electric vehicles and offshore wind farms connected to the grid through an HVDC link was presented in [27]. It has been shown that the uncertainty associated with availability of power from wind farm and PEVs affects the overall cost of operation of system. Lin and Lin [28] proposed a risk-limiting optimal power flow (RLOPF) problem for systems with high wind power penetration; the aim was to address the issue of possibly violating the security constraints in power systems due to the instability of wind power generations.

3. Optimal Power Flow

3.1. OPF of Conventional Power Grid

Load flow, also known as a power flow, is a network solution that displays currents, voltages, and real and reactive power flows at each bus and lines in the power system. The calculation of power flow necessitates the solution of non-linear equations. It can calculate the transmission system's electrical response to a specific set of loads and generator power outputs. Carpentier presented Optimal Power Flow in 1962 [4]. The OPF is typically a non-linear and non-convex problem with Objective Function that must be optimized (maximized or minimized), a set of equality and inequality constraints that must be satisfied, and a problem-solving method. Specifically, OPF optimizes a given Objective Function controlling power flow throughout an electrical system without violating power flow constraints or operational limits [4]. In other words, each power plant's actual and reactive power should be scheduled so that the total operating cost is kept to a minimum. Thus, it can help grid operators address various challenges in grid planning, operation, and control. OPF can also be used to determine prices on the day-ahead market [29]. Some of the extended OPF versions are illustrated below [4]:

- SCOPF: It selects the optimal control settings for the base system to minimize the objective function while ensuring that no violations occur.
- DC OPF: The reactive power and transmission losses are not taken into account.
- AC OPF: It has to do with the AC grid and is based on the system's natural PF characteristics. As a result, the outputs of this type of OPF are more precise.
- Mixed AC/DC OPF: it is related to the OPF in both AC and DC grids.

OPF has been solved using a variety of conventional optimization methods such as Linear Programming method, Non-linear Programming method, Quadratic Programming method, Newton's method, and Interior Point method [30]. However, all of these methods have their own set of benefits and drawbacks which will be discussed further.

3.2. OPF Problem Formulation

- The following is a description of a general minimization problem:
- Minimize: $f(x,u)$ (the objective function) where $f(x,u)$ is the objective function.
- Subject to: $h_i(x,u) = 0, i = 1,2,3,\dots, m$ (equality constraints) where $h_i(x,u)$ is set of equality constraints.
- $g_j(x,u) \leq 0, j = 1,2,3, \dots, n$ (inequality constraints) where $g_j(x,u)$ is set of inequality constraints, u represents a set of controllable and x represents dependent variables.

3.3. Objective function

These objective functions vary from fuel cost generation, active and reactive power transmission loss, reactive power reserve margin, security margin index, and emission environmental index [31].

3.3.1. Minimization of Generation Fuel Cost

The key objective of the OPF solution is to reduce the system's total operating costs. When there is a light load, the cheapest generators are always chosen to run first. More expensive generators will be brought in as the load increases. As a result, the operational cost plays a critical

part in the OPF solution. The amount of fuel or input to a generator is usually measured in British thermal units per hour (Btu/hr) and the output in megawatts (MW) [30].

In all practical cases, the cost of generator i can be shown as a function of real power generation,

$$C_i = [a_i + (b_i P_i) + (c_i P_i^2)] * \text{fuel cost} \quad (3.1)$$

which is expressed in expressed in \$/hr

Where P_i is the real power output of generator i , and a_i , b_i , c_i are the cost coefficients.

The incremental cost can be obtained from the derivative of C_i with respect to P_i ,

$$dC_i/dP_i = (b_i + 2c_i P_i) * \text{fuel cost} \quad (3.2)$$

which is expressed in \$/MWhr.

3.3.2. Minimization of Active Power Transmission Loss

The OPF problem goal is to minimize the power loss. The formulation of the real power loss can be represented by [31]:

$$\text{Minimizing } P_{\text{Loss}} = \sum P_i = \sum P_{gi} - \sum P_{di}, i = 1, \dots, N_b \quad (3.3)$$

where P_{Loss} is the total I²R loss in the transmission lines and transformers of the network.

3.3.3. Minimization of Reactive Power Transmission Loss

The total VAR loss is minimized as per the following equation [31]:

$$\text{Minimizing } Q_{\text{Loss}} = \sum Q_{gi} - \sum Q_{di}, i = 1, \dots, N_b \quad (3.4)$$

3.4. Control and Dependent Variables

There are two relevant variables in an optimization problem: independent/control variables and dependent/state ones. Firstly, the optimal value must be determined for control variables to help minimize the objective function, and then, based on it, state variables should be calculated [4].

In the OPF problem, control variables may include active power generation of all generator buses except slack bus, the voltage of all generator buses, transformers tap ratio, reactive power injection of shunt capacitor banks, etc. Moreover, dependent variables may also include an active

power output of the slack bus, voltage angles of all buses excluding the slack bus, load bus voltages, reactive power generation of generators. It should be noted that the number of control variables determines the solution space. In fact, a problem with n -control variables results in an n -dimensional solution space [4]. The classification of power system buses is shown in Table 3.1 [31].

Table – 3.1: Classification of Power System Buses.

Classifications	Knowns	Unknowns
Load Bus	P, Q	V, δ
Generator Bus	P, V	Q, δ
Slack (Swing) bus	V, δ	P, Q

3.5. Equality constraints

Both the physicality of the power system and the required voltage set points are reflected in the OPF's equality constraints. The power system physics is enforced by power flow equations that require that actual and reactive power injection for each bus amount to zero [30].

This can be attained by the following analysis:

$$P_i = P_{\text{Load}} + P_{\text{Loss}} \quad (3.5)$$

$$Q_i = Q_{\text{Load}} + Q_{\text{Loss}} \quad (3.6)$$

where P_i and Q_i are the active and reactive power outputs respectively.

P_{Load} and Q_{Load} are the active and reactive load power respectively.

P_{Loss} and Q_{Loss} are the active and reactive power loss respectively.

The power flow equations of the network can be given as:

$$G(V, \delta) = 0 \quad (3.7)$$

where

$$G(V, \delta) = P_i(V, \delta) - P_i^{\text{net}}, Q_i(V, \delta) - Q_i^{\text{net}}, P_m(V, \delta) - P_m^{\text{net}} \quad (3.8)$$

where P_i and Q_i are the calculated real and reactive power at PQ bus respectively

P_i^{net} and Q_i^{net} are the specified real and reactive power for PQ bus respectively

V and δ are the magnitude and phase angle of voltage at different buses respectively

3.6. Inequality constraints

Components and equipment in the power system have operational limitations created to ensure system security and minimize the required objective function [30].

Inequality constraints:

$$P_{gi}^{\min} \leq P_{gi} \leq P_{gi}^{\max} \quad (3.9)$$

$$Q_{gi}^{\min} \leq Q_{gi} \leq Q_{gi}^{\max} \quad (3.10)$$

$$\Sigma P_{gi} - P_D - P_{Loss} = 0 \quad (3.11)$$

where P_{gi} is the amount of generation in MW at generator i .

Q_{gi} is the amount of generation in MVAR at generator i .

The inequality constraints on voltage magnitude V of each PQ bus

$$V_i^{\min} \leq V_i \leq V_i^{\max} \quad (3.12)$$

where V_i^{\min} and V_i^{\max} are the minimum and maximum values of voltages at bus i .

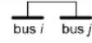
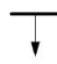


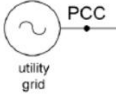
The inequality constraints on phase angle δ of voltages at all buses i

$$\delta_i^{\min} \leq \delta_i \leq \delta_i^{\max} \quad (3.13)$$

where δ_i^{\min} and δ_i^{\max} are the minimum and maximum values of phase angle at bus i .

For a typical Microgrid system, the basic components are given in Table 3.2 [12]:

Table - 3.1 Typical Microgrid components.

Unit	Symbol	Constraints
power line		Constraints: $I_{i,j,x}(t) < I_{i,j,max}$
load		Constraints: $P_{i,x}(t) = -P_{L,i,x}(t)$ (fixed) $Q_{i,x}(t) = -Q_{L,i,x}(t)$ (fixed) $V_{i,x,min} \leq V_{i,x}(t) \leq V_{i,x,max}$ Free variables: $V_{i,x}(t), \delta_{i,x}(t)$
Renewable generator		Constraints: $P_{i,x}(t) = +P_{g,i,x}(t)$ (fixed) $Q_{i,x}(t) = +Q_{g,i,x}(t)$ (fixed) $V_{i,x,min} \leq V_{i,x}(t) \leq V_{i,x,max}$ Free variables: $V_{i,x}(t), \delta_{i,x}(t)$
storage device		$E_{i,x}(t)$ = stored energy or state of charge (SOC). Typical constraints: $V_{i,x}(t) = V_{S,i}$ (fixed) $0 \leq E_i(t) \leq E_{i,max}$ $-P_{i,rated} \leq P_i(t) \leq +P_{i,rated}$ State equation (one-phase): $\frac{d}{dt} E_i = f_i(P_i, E_i)$ Free variables: $P_i(t), Q_i(t), \delta_i(t), E_i(t)$
point of common coupling (PCC)		The PCC is always indexed as bus 1, $i=1$. Constraints: $\delta_{1,x}(t) = 0$ $V_{1,x}(t) = V_{in,x}$ (fixed) $Q_{1,x,min} \leq Q_{1,x}(t) \leq Q_{1,x,max}$ $P_{1,x,min} \leq P_{1,x}(t) \leq P_{1,x,max}$ Free variables: $P_1(t), Q_1(t)$

Where the PCC corresponds to the "slack" bus. It is always indexed as bus 1.

3.7. Conventional Vs Recent Optimization Methods for OPF

The Conventional methods are based on linear Objective Functions that apply sensitivity analysis and gradient-based optimization algorithms. The conventional optimization methods are illustrated below [32]:

3.7.1. Linear Programming method

LP method is one of the fully developed methods now in common use. It easily handles inequality constraints. Non-linear objective functions and constraints are handled by linearization [33]. LP method is used for linearizing the problems of non-linear system optimization; it is reliable. It has a good convergence feature, but the main shortcoming is that errors may occur due to digital computer rounding, especially under constraints.

3.7.2. Non-Linear Programming method

NLP is a process of solving an optimization problem where the constraints and the OF are non-linear. It helps to find the best solution to a problem using constraints that are not linear. The non-linear method (NLP) is more precise

than the linear method, where non-linear objective functions and constraints can be applied. The NLP techniques use the Lagrange multiplier to use the reduced gradient method. The significance of this method is that it can be applied in a large-scale system, whereas the disadvantages are that some system components are not taken into consideration [32].

3.7.3. Quadratic Programming method

A particular nonlinear programming approach can be seen in quadratic programming (QP), where the objective function is quadratic, and the constraints are linear. The determination of gradient steps is not necessary for this method. The solution that has been obtained using the QP Method is more accurate compared to the previous methods. In addition, it has fast convergence characteristics [32].

3.7.4. Newton's method

The Newton Method is commonly used in power flow problems by applying second-order partial derivatives to create the Lagrangian. It is a high-speed convergence method, but it may give problems with inequality constraints. It was proved that Newton-Raphson converged in many cases. Moreover, most Newton-Raphson power flow problems converge in less than ten iterations. The disadvantages are that the Newton-Raphson method requires high computer storage and computation time, and it is very much sensitive to the selection of initial conditions [33].

3.7.5. Interior Point method

IP method is one of the fully developed and widely used methods for OPF. The IP method is generally used for large problems to solve the optimal power problem [32]. However, the results achieved by IP results are better and require fewer iterations than LP. It easily handles inequality constraints [33].

The conventional methods are not always appropriate for optimizing the power flow since the optimal power flow is a non-linear (non-convex) problem. Therefore, new optimization methods are introduced to solve the OPF. The advantages of these recent methods are the following [32]:

1. They can be applied in small and large scale systems
2. It has a high reliability

3. They converge rapidly compared to the conventional methods.

The recent optimization methods can be classified as follows [32]:

- Swarm and Bio-inspired Optimization Techniques

The natural and bio-inspired algorithm is an emerging approach based on the inspiration of the moving and looking behavior of animals or birds for food sources.

- Human-Inspired Optimization Techniques

Various techniques of optimization simulate human behavior, particularly when it comes to thinking or making decisions.

- Physics-Inspired Optimization Techniques

Algorithms based on physics are conceptualized in space through physics laws or natural phenomena.

- Evolutionary-Inspired Optimization Techniques

Evolutionary optimization algorithms come from natural selection mechanics and genetics or living bodies or animals.

- Hybrid Optimization Techniques

Several algorithms have been proposed for hybrid optimization to gain advantages of multiple techniques and obtain better results than single techniques.

- Artificial Neural Network (ANN) and Fuzzy Logic Approach

Artificial neural networks (ANNs) are computational methods that emulate the operation of biological neural networks. At the same time, the fuzzy set theory is a natural and appropriate tool for inaccurate relations.

4. Networked Microgrid Test System

A Microgrid can connect with the main grid by a DG control entity to serve local loads. The balance between the generation and load must be kept under all operating conditions to keep the frequency and voltage of MGs within operating limits. These DGs may be dispatchable or non-dispatchable. For example, the power generation from PV panels and wind turbines is usually non-dispatchable. In contrast, the power output from the microturbines, fuel cells, combined heat and power (CHP), and diesel generators are fully dispatchable. The grid, which serves as

the MG's slack bus, handles this balance in grid-connected mode. While in an islanded mode, dispatchable DG must have sufficient capacity to balance load and generation and avoid load shedding.

Figure 4.1 shows the electrical single-line diagram of the test system with comprehensive buses, loads, and generation. A three-digit number is used to identify each bus in the system. All lines, including the tie lines, are underground cables. Table 4.1 shows more details on the four microgrids [34].

The first bus of each microgrid (101, 201, 301, and 401) serves as the slack bus of that microgrid, and its equipped with two or three units of conventional Synchronous Generators to allow the microgrid to function effectively in isolated mode, with load balancing and reactive power supported. While in grid-connected mode, the slack bus of microgrid 1 (101) is the slack bus on the complete system [34]. Load and generation balance is performed through this bus.

As shown in Table 4.1, microgrid 1 consists of 6 buses, 11 underground cables, and three standby Synchronous Generators, each of 5000 kVA connected to bus 101. Moreover, 3 PV panels are installed at buses 102, 103, and 104. microgrid 2 consists of 9 buses, eight underground cables, and three standby Synchronous Generators at bus 201. Additionally, 3 PV panels (at buses 202, 203, and 204) and 2 Wind Turbines (at buses 206 and 209) are always available to generate power to the network. microgrid 3 has 18 buses and 17 underground cables. Bus 301 has three standby Synchronous Generators and 6 PV panels (at buses 303, 304, 305, 306, 307, and 315) and 2 Wind Turbines (at buses 314 and 317). Finally, microgrid 4 has seven buses and eight underground cables, 3 PV panels at (at buses 405, 406, and 407), and two standby Synchronous Generators installed at bus 401. All these standby SGs are of equal capacity and have self-starting capability [34].

The networked microgrid system is designed to operate on 11 kV three-phase underground cables. The utility feeder is a 33 kV three-phase single circuit overhead line. In

addition, there are three 20 MVA parallel step-down transformers to maintain the voltage of 11 kV at bus 101.

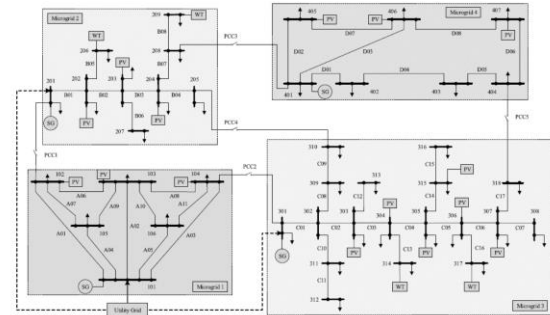


Fig - 4.1 Single-line diagram of the Networked MGs test system.

As shown in Figure 4.1, microgrid 1 can share power with microgrid 2 through PCC1 and microgrid 3 through PCC2. While microgrid 2 can share power with microgrid 3 through PCC4 and microgrid 4 with PCC3. microgrid 3 and microgrid 4 can exchange power through PCC5. If a failure occurs in microgrid 1, microgrid 2 and 3 can be connected to the utility grid directly to ensure the continuity of supply.

Table - 4.1 Details of Microgrids of the test system.

Components	MG 1	MG 2	MG 3	MG 4
Buses	6	9	18	7
Lines	11	8	17	8
SGs	3	3	3	2
PV Systems	3	3	6	3
WT Systems	0	2	2	0
Slack Bus	101	201	301	401
MG Type	Meshed	Radial	Radial	Meshed

The line and bus data are necessary to perform out an optimal power flow analysis. The data from the networked microgrid system lines such as resistance, reactance, and cable length is presented in Table 4.2 [34]. Moreover, Table 4.3 shows the tie-cable data between the microgrids [34].

Table - 4.2 Line Data of the Networked MG System.

S. No.	From Bus	To Bus	Length (km)	Resistance (P.U)	Reactance (P.U)
1	101	102	3	0.7661	1.18
2	101	103	2.4	0.7715	0.991
3	101	104	3	0.7661	1.18
4	101	105	1.6	0.514	0.6604
5	101	106	1.6	0.514	0.6604
6	102	103	2	0.6429	0.825
7	102	105	1.5	0.4822	0.619
8	103	104	2	0.6429	0.825
9	103	105	1.2	0.3857	0.495
10	103	106	1.2	0.3857	0.495
11	104	106	1.5	0.4822	0.619
12	201	202	1.4	0.4500	0.577
13	202	203	1.6	0.5143	0.660
14	202	206	1.5	1.9710	1.338
15	203	204	2.2	0.7072	0.908
16	203	207	1.4	1.8396	1.249
17	204	205	1.8	0.5786	0.743
18	204	208	1.2	0.3857	0.495
19	208	209	0.8	1.0512	0.714
20	301	302	1.2	0.3857	0.495
21	302	303	1.8	0.5786	0.743
22	302	309	1.5	0.4822	0.619
23	302	311	1.4	1.8396	1.249

24	303	304	1.2	0.3857	0.495
25	303	313	1.5	1.9710	1.338
26	304	305	1.4	0.4500	0.577
27	304	314	1.4	1.8396	1.249
28	305	306	1.6	0.5143	0.660
29	305	315	1.4	1.8396	1.249
30	306	307	1.5	0.4822	0.619
31	306	317	1.4	1.8396	1.249
32	307	308	1.5	1.9710	1.338
33	307	318	1.7	0.5465	0.701
34	309	310	1.5	0.4822	0.619
35	311	312	1.2	1.5768	1.071
36	315	316	1.2	1.5768	1.071
37	401	402	0.6	0.3148	0.260
38	401	405	1	0.5247	0.433
39	401	406	1.8	0.9446	0.780
40	402	403	2	1.0495	0.867
41	403	404	0.6	0.3148	0.260
42	404	407	1	0.5247	0.433
43	405	406	1.5	0.7871	0.650
44	406	407	1.5	0.7871	0.650

Table - 4.3 PCC/Tie-cables Data.

S. No.	From bus	To Bus	Length (km)	Resistance (P.U)	Reactance (P.U)
T1	102	201	1	0.2553	0.394
T2	104	301	1.5	0.3830	0.591
T3	208	401	2	0.6429	0.825
T4	205	310	2.5	0.8037	1.032

T5	318	404	1	0.3214	0.412
----	-----	-----	---	--------	-------

A one-year dataset has been provided in this system. Table 4.4 provides the load data for the Networked Microgrids [34]. Table 4.4 indicates that the overall system loads are 30.802 MW and 6.374 MW, including critical loads of 6.16 MW and 1.27 MVAR. In addition, the table lists three types of buses: 1) Type 1 bus: Slack bus; 2) Type 2 bus: Generator bus; 3) Type 3 bus: Load bus (PQ bus).

Table - 4.4 Load Data of the Networked MG System.

Bus ID	Bus Type	Total Bus Load kW	Total Bus Load kVAR	Critical Load kW	Critical Load kVAR	Bus Load % of System Load
101	1	0	0	0	0	0
102	2	2125	336	450	68	6.9
103	2	3329	1023	650	124	10.81
104	2	2050	555	200	50	6.66
105	3	1257	310	200	35	4.08
106	3	1056	240	200	35	3.43
201	2	600	100	0	0	1.95
202	2	1250	487	500	80	4.06
203	2	1203	410	500	80	3.91
204	2	1366	443	650	138	4.43
205	3	764	36	0	0	2.48
206	2	503	21	0	0	1.63
207	3	345	11	0	0	1.12
208	3	629	8	0	0	2.04
209	2	642	12	100	25	2.08
301	2	580	150	0	0	1.88
302	3	650	85	250	50	2.11
303	2	673	96	0	0	2.18
304	2	439	135	0	0	1.43
305	2	600	128	250	50	1.95
306	2	560	112	0	0	1.82
307	2	851	145	385	50	2.76
308	3	420	25	0	0	1.36
309	3	500	45	0	0	1.62
310	3	637	33	0	0	2.07
311	3	788	95	350	83	2.56
312	3	125	50	0	0	0.41
313	3	169	20	0	0	0.55
314	2	200	43	0	0	0.65
315	2	250	32	125	25	0.81
316	3	213	12	0	0	0.69
317	2	133	25	0	0	0.43
318	3	200	38	0	0	0.65
401	2	426	80	0	0	1.38
402	3	318	78	125	20	1.03

403	3	356	81	125	20	1.16
404	3	459	88	0	0	1.49
405	2	820	91	0	0	2.66
406	2	2500	635	850	150	8.12
407	2	816	60	250	44	2.65
Total Load		30802	6374	6160	1127	100

Base voltage: 11 kV; Specified voltage at all buses: 1 p.u.

Table 4.5 presents details of DERs installed at different MG locations. Excess power is saved in energy storage systems installed with each PV system to use the stored energy when the PV solar is unavailable. Also, the details of the Synchronous Generators are presented in Table 4.6 [34].

Table - 4.5 Installed Capacity of PV and WT in MGs.

Bus ID	DG Type	PG (kW)	QGmin (kVAR)	QGmax (kVAR)	Network Area
102	PV	2000	0	400	MG1
103	PV	2400	0	480	MG1
104	PV	2000	0	400	MG1
202	PV	1600	0	320	MG2
203	PV	1600	0	320	MG2
204	PV	2400	0	480	MG2
206	WT	800	-250	250	MG2
209	WT	500	-200	200	MG2
303	PV	2000	0	500	MG3
304	PV	400	0	100	MG3
305	PV	800	0	160	MG3
306	PV	800	0	160	MG3
307	PV	800	0	160	MG3
314	WT	500	-250	250	MG3
315	PV	800	0	160	MG3
317	WT	1200	-600	600	MG3
405	PV	1600	0	320	MG4
406	PV	2400	0	500	MG4
407	PV	1600	0	320	MG4

Table - 4.6 Standby Synchronous Generators Data in MGs

Bus ID	Unit Capacity (kVA)	Number of Units	QGmin (kVAR)	QGmax (kVAR)	Network area
101	5000	3	-3000	5000	MG1
201	2000	3	-1500	2000	MG2
301	2000	3	-1500	2000	MG3
401	2000	2	-1000	2000	MG4

The Energy Storage Systems are installed at different buses, which are Lithium-ion batteries. With 80% of DOD.

The SoC of batteries is assumed to be 20% of their total capacity. The details of the ESS are shown in Table 4.7 [34].

Table - 4.7 Energy Storage Capacity.

Location (Bua ID)	Battery Storage Capacity (kWh)	Peak Power Supply (Kw)	Network Area
102	3000	2000	MG1
103	4000	2400	MG1
104	3000	2000	MG1
202	4000	1600	MG2
203	4000	1600	MG2
204	4000	2400	MG2
303	3600	2000	MG3
304	800	400	MG3
305	2000	800	MG3
306	2000	800	MG3
307	2000	800	MG3
315	2000	800	MG3
405	3000	1600	MG4
406	6000	2400	MG4
407	3000	1600	MG4

5. OPF in Microgrids using Newton-Raphson method

For the networked microgrids illustrated in the previous chapter, an Optimal Power Flow study will be performed using Newton-Raphson method.

5.1. Principle of Newton-Raphson method

A nonlinear equation in a single variable can be expressed as:

$$f(x) = 0 \quad (5.10)$$

For solving this equation, select an initial value x_0 . The difference between the initial value and the final solution is Δx . Then $x_1 = x_0 + \Delta x$ is the solution of nonlinear equation (5.10). That is [35]:

$$f(x_0 + \Delta x) = 0 \quad (5.11)$$

Expanding the above equation with the Taylor series yields [35]:

$$f(x_0 + \Delta x) = f(x_0) + f'(x_0) \Delta x + \frac{f''(x_0)(\Delta x)^2}{2!} + \dots + \frac{f^{(n)}(x_0)(\Delta x)^n}{n!} + \dots = 0 \quad (5.12)$$

where $f'(x_0), \dots, f^{(n)}(x_0)$ are the derivatives of the function $f(x)$.

If the difference Δx is very small (meaning that the initial value x_0 is close to the solution of the function), the terms of the second and higher derivatives can be neglected. Thus equation (5.12) becomes a linear equation as below [35]:

$$f(x_0 + \Delta x) = f(x_0) + f'(x_0) \Delta x = 0 \quad (5.13)$$

Then:

$$\Delta x = -f(x_0)/f'(x_0) \quad (5.14)$$

The new solution will be:

$$x_1 = x_0 + \Delta x = x_0 - f(x_0)/f'(x_0) \quad (5.15)$$

Since equation (5.13) is an approximate equation, the value of Δx is also an approximation.

Thus the solution x is not a real solution. Further iterations are needed. The iteration equation is [35]:

$$x_{k+1} = x_k + \Delta x_k = x_k - f(x_k)/f'(x_k) \quad (5.16)$$

The iteration can be stopped if one of the following conditions is met:

$$|\Delta x_k| < \epsilon_1 \text{ or } |f(x_k)| < \epsilon_2 \quad (5.17)$$

where ϵ_1, ϵ_2 , which are the permitted convergence precisions, are small positive numbers.

The Newton method can also be expanded to a nonlinear equation with n variables.

$$f_1(x_1, x_2, \dots, x_n) = 0$$

$$f_2(x_1, x_2, \dots, x_n) = 0$$

...

$$f_n(x_1, x_2, \dots, x_n) = 0$$

For a given set of initial values x_1, x_2, \dots, x_n , we have the corrected values $\Delta x_1, \Delta x_2, \dots, \Delta x_n$. Then:

$$f_1(x_1 + \Delta x_1, x_2 + \Delta x_2, \dots, x_n + \Delta x_n) = 0$$

$$f_2(x_1 + \Delta x_1, x_2 + \Delta x_2, \dots, x_n + \Delta x_n) = 0$$

...

$$f_n(x_1 + \Delta x_1, x_2 + \Delta x_2, \dots, x_n + \Delta x_n) = 0$$

Similarly, expanding the above equations and neglecting the terms of second and higher derivatives, a matrix can be formed to find the solution at kth iteration [35]:

$$\begin{bmatrix} f_1(x_1^k, x_2^k, \dots, x_n^k) \\ f_2(x_1^k, x_2^k, \dots, x_n^k) \\ \dots \\ f_n(x_1^k, x_2^k, \dots, x_n^k) \end{bmatrix} = - \begin{bmatrix} \frac{\partial f_1}{\partial x_1} \Big|_{x_1^k} & \frac{\partial f_1}{\partial x_2} \Big|_{x_2^k} & \dots & \frac{\partial f_1}{\partial x_n} \Big|_{x_n^k} \\ \frac{\partial f_2}{\partial x_1} \Big|_{x_1^k} & \frac{\partial f_2}{\partial x_2} \Big|_{x_2^k} & \dots & \frac{\partial f_2}{\partial x_n} \Big|_{x_n^k} \\ \vdots & \vdots & \ddots & \vdots \\ \frac{\partial f_n}{\partial x_1} \Big|_{x_1^k} & \frac{\partial f_n}{\partial x_2} \Big|_{x_2^k} & \dots & \frac{\partial f_n}{\partial x_n} \Big|_{x_n^k} \end{bmatrix} \begin{bmatrix} \Delta x_1^k \\ \Delta x_2^k \\ \vdots \\ \Delta x_n^k \end{bmatrix}$$

$$x_{k+1i} = x_{ki} + \Delta x_{ki} \quad i = 1, 2, \dots, n \quad (5.18)$$

The above two equations can be expressed as

$$F(X_k) = -J_k \Delta X_k \quad (5.19)$$

$$X_{k+1} = X_k + \Delta X_k \quad (5.20)$$

where J is an n × n matrix called a Jacobian matrix.

5.2. Power Flow Solution

The complex voltage, real and reactive powers of each bus:

$$V_i = V_i(\cos \theta_i + j \sin \theta_i) \quad (5.21)$$

$$P_i = V_i \sum_{j=1}^n V_j (G_{ij} \cos \theta_{ij} + B_{ij} \sin \theta_{ij}) \quad (5.22)$$

$$Q_i = V_i \sum_{j=1}^n V_j (G_{ij} \sin \theta_{ij} - B_{ij} \cos \theta_{ij}) \quad (5.23)$$

where $\theta_{ij} = \theta_i - \theta_j$, which is the angle difference between buses i and j.

For each PV or PQ bus, we have the following real power mismatch equation:

$$\Delta P_i = P_{is} - P_i = P_{is} - V_i \sum_{j=1}^n V_j (G_{ij} \cos \theta_{ij} + B_{ij} \sin \theta_{ij}) = 0 \quad (5.24)$$

For each PQ bus, we also have the following reactive

$$\Delta Q_{is} = Q_{is} - Q_i = Q_{is} - V_i \sum_{j=1}^n V_j (G_{ij} \sin \theta_{ij} - B_{ij} \cos \theta_{ij}) = 0$$

power equation:

$$(5.25)$$

where P_{is} , Q_{is} are the calculated bus real and reactive power injections, respectively.

According to the Newton method, the power flow equations (5.24) and (5.25) can be expanded into Taylor series and the following first-order approximation can be obtained [35]:

$$\begin{bmatrix} \Delta P \\ \Delta Q \end{bmatrix} = -J \begin{bmatrix} \Delta \theta \\ \Delta V/V \end{bmatrix} \quad (5.26)$$

where

$$\Delta P = \begin{bmatrix} \Delta P_1 \\ \Delta P_2 \\ \vdots \\ \Delta P_{n-1} \end{bmatrix} \quad \Delta Q = \begin{bmatrix} \Delta Q_1 \\ \Delta Q_2 \\ \vdots \\ \Delta Q_m \end{bmatrix} \quad (5.27)$$

$$\Delta \theta = \begin{bmatrix} \Delta \theta_1 \\ \Delta \theta_2 \\ \vdots \\ \Delta \theta_{n-1} \end{bmatrix} \quad \Delta V = \begin{bmatrix} \Delta V_1 \\ \Delta V_2 \\ \vdots \\ \Delta V_m \end{bmatrix}$$

The steps for calculation of the Newton-power flow solution are shown in the following flowchart:

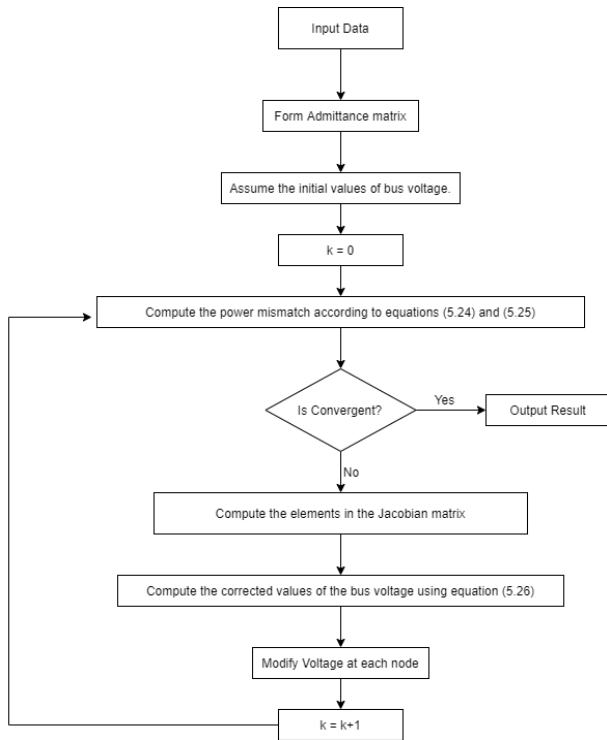


Fig - 5.1 FlowChart of Newton-Raphson method.

5.3. Power Flow Results using Newton-Raphson method

After applying the Newton-Raphson method to the networked microgrids, the results are shown in the following sections:

5.3.1. Using Storage as a load:

Using the line and bus data provided in the previous chapter for the networked microgrids, the power flow solution is obtained using the Newton-Raphson method with MATLAB computations. This yields the results shown in Table 5.1. Note that for more accessible dealing with numbers, the three-digit numbers for buses from 101 to 407 are described as 1 to 40 buses.

Table - 5.1 Power Flow Results using Newton-Raphson – Storage as Load.

Bus No.	Voltage Mag.	Angle Degree	-----Load-----		---Generation---		Injected Mvar
			MW	Mvar	MW	Mvar	
1	1.000	0.000	0.000	0.000	13.862	-2.997	0.000
2	0.980	-1.452	4.125	0.336	2.000	-7.052	0.000
3	0.990	-1.837	5.729	1.023	2.400	4.305	0.000
4	0.990	-2.327	4.050	0.555	2.000	1.329	0.000
5	0.987	-1.288	1.257	0.310	0.000	0.000	0.000
6	0.991	-1.545	1.056	0.240	0.000	0.000	0.000
7	1.000	-2.520	0.600	0.100	6.000	6.193	0.000
8	0.970	-4.579	2.850	0.487	1.600	-1.654	0.000
9	0.950	-7.010	2.803	0.410	1.600	-0.971	0.000
10	0.950	-10.158	3.766	0.443	2.400	-0.769	0.000
11	0.947	-9.620	0.764	0.036	0.000	0.000	0.000
12	0.990	-5.581	0.503	0.021	0.800	1.074	0.000
13	0.943	-7.273	0.345	0.011	0.000	0.000	0.000
14	0.965	-12.068	0.629	0.008	0.000	0.000	0.000
15	0.970	-12.692	0.642	0.012	0.500	0.885	0.000
16	0.990	-3.652	0.580	0.150	6.000	0.959	0.000
17	0.964	-6.285	0.650	0.085	0.000	0.000	0.000
18	0.950	-8.385	2.673	0.096	2.000	-0.922	0.000
19	0.950	-9.794	0.839	0.135	0.400	0.031	0.000
20	0.950	-11.322	1.400	0.128	0.800	0.357	0.000
21	0.950	-12.318	1.360	0.112	0.800	-0.963	0.000
22	0.950	-13.534	1.651	0.145	0.800	-0.568	0.000
23	0.941	-13.863	0.420	0.025	0.000	0.000	0.000
24	0.956	-7.420	0.500	0.045	0.000	0.000	0.000
25	0.950	-8.390	0.637	0.033	0.000	0.000	0.000
26	0.945	-6.834	0.788	0.095	0.000	0.000	0.000
27	0.942	-6.870	0.125	0.050	0.000	0.000	0.000
28	0.946	-8.504	0.169	0.020	0.000	0.000	0.000
29	0.960	-9.937	0.200	0.043	0.500	0.370	0.000
30	0.950	-12.506	1.050	0.032	0.800	0.743	0.000
31	0.946	-12.639	0.213	0.012	0.000	0.000	0.000
32	0.980	-12.383	0.133	0.025	1.200	0.807	0.000
33	0.963	-14.587	0.200	0.038	0.000	0.000	0.000
34	0.990	-14.405	0.426	0.080	4.000	3.574	0.000
35	0.985	-14.578	0.318	0.078	0.000	0.000	0.000
36	0.974	-15.047	0.356	0.081	0.000	0.000	0.000
37	0.972	-15.148	0.459	0.088	0.000	0.000	0.000
38	0.980	-14.851	2.420	0.091	1.600	-1.151	0.000
39	0.980	-15.792	4.900	0.635	2.400	2.464	0.000
40	0.980	-16.072	2.416	0.060	1.600	2.908	0.000
Total			54.002	6.374	56.062	8.954	0.000

In the first case where the storage systems are considered as loads, the ESS, which is installed next to each PV system, will absorb the generated power and store it in the batteries—assuming that from 6 A.M to 6 P.M, the energy from the sunlight is absorbed by the PV cells in the panel to produce electricity. Wind Turbine, the PV system, and the synchronous generators units are operating, the batteries are charged from the PV system. The calculations through MATLAB Software has convincing results:

- A constant voltage for nodes such as 1 and 7, and a particular variation limit for others.
- The balance of the system is ensured as the loads should be equal to the generated power from the sources. As shown in Table 5.1, the load is designed to be 54.002 MW, while the generation is 56.062 MW.
- The losses are calculated to be 2.065 MW/ 2.582 MVAR due to cable length, resistance, and reactance.
- The execution time is 1.263629 seconds.
- The number of iterations is 11.
- Maximum Power Mismatch = 1.15132e-05.

5.3.2. Using Storage as a source:

In the second case, from 6 P.M to 6 A.M, the ESS is considered to be a source that can generate power to maintain system balance and reliability when the PV system is not operating while wind turbines and synchronous generators units are operating. The batteries are discharging with a DOD of 80%. Table 5.2 illustrates the power flow results when the batteries are discharging.

The following are observed from the power flow output:

A constant voltage for multiple nodes and a certain variation limit for others.

As shown in Table 5.2, the load is designed to be 30.802 MW, while the generation is 31.697 MW.

The losses are calculated to be 0.896 MW/1.149 MVAR due to the cable length, cable resistance, and reactance

The execution time is 1.032611 seconds.

The number of iterations till convergence is 10.

Maximum Power Mismatch = 1.98777e-06.

Table - 5.2 Power flow Results using Newton-Raphson - Storage as Source.

Bus No.	Voltage Mag.	Angle Degree	-----Load-----		---Generation---		Injected Mvar
			MW	Mvar	MW	Mvar	
1	1.000	0.000	0.000	0.000	-5.863	2.256	0.000
2	1.010	1.312	2.125	0.336	1.600	6.631	0.000
3	1.000	0.667	3.329	1.023	1.920	-0.615	0.000
4	1.010	1.074	2.050	0.555	1.600	5.938	0.000
5	1.001	0.562	1.257	0.310	0.000	0.000	0.000
6	1.001	0.504	1.056	0.240	0.000	0.000	0.000
7	1.000	3.566	0.600	0.100	6.000	-3.905	0.000
8	0.990	4.362	1.250	0.487	1.280	-0.282	0.000
9	0.990	4.586	1.203	0.410	1.280	0.639	0.000
10	0.990	5.126	1.366	0.443	1.920	-0.731	0.000
11	0.985	4.439	0.764	0.036	0.000	0.000	0.000
12	0.980	5.928	0.503	0.021	0.800	-1.122	0.000
13	0.983	4.344	0.345	0.011	0.000	0.000	0.000
14	0.997	5.449	0.629	0.008	0.000	0.000	0.000
15	1.000	5.036	0.642	0.012	0.500	0.598	0.000
16	1.000	3.791	0.580	0.150	6.000	-3.460	0.000
17	0.993	3.931	0.650	0.085	0.000	0.000	0.000
18	1.000	4.841	0.673	0.096	1.600	2.560	0.000
19	0.990	5.777	0.439	0.135	0.320	-0.593	0.000
20	0.980	6.733	0.600	0.128	0.640	-2.941	0.000
21	0.990	6.730	0.560	0.112	0.640	1.506	0.000
22	0.990	6.503	0.851	0.145	0.640	0.751	0.000
23	0.981	6.200	0.420	0.025	0.000	0.000	0.000
24	0.987	3.845	0.500	0.045	0.000	0.000	0.000
25	0.984	3.928	0.637	0.033	0.000	0.000	0.000
26	0.974	3.413	0.788	0.095	0.000	0.000	0.000
27	0.971	3.380	0.125	0.050	0.000	0.000	0.000
28	0.996	4.734	0.169	0.020	0.000	0.000	0.000
29	1.000	5.612	0.200	0.043	0.500	0.402	0.000
30	0.980	7.147	0.250	0.032	0.640	-0.213	0.000
31	0.976	7.021	0.213	0.012	0.000	0.000	0.000
32	1.000	8.291	0.133	0.025	1.200	-0.716	0.000
33	0.989	6.690	0.200	0.038	0.000	0.000	0.000
34	1.010	6.550	0.426	0.080	4.000	2.833	0.000
35	1.005	6.569	0.318	0.078	0.000	0.000	0.000
36	0.992	6.748	0.356	0.081	0.000	0.000	0.000
37	0.990	6.841	0.459	0.088	0.000	0.000	0.000
38	1.010	6.532	0.820	0.091	1.280	2.663	0.000
39	0.990	7.494	2.500	0.635	1.920	-4.207	0.000
40	0.990	7.270	0.816	0.060	1.280	-0.471	0.000
Total			30.802	6.374	31.697	7.522	0.000

6. OPF in Microgrids using Neural-Network method

After applying the Neural-Network method to the networked microgrids, the results are shown in the following sections:

6.1. Principle of Neural Network method

The evolutionary computing of Artificial Intelligence is solely entering the world and spreading the idea that it is easier and more intelligent than the conventional methods in performing complex tasks. The Neural Network displays spatial capacities based on human logic.

Neural networks are a subset of machine learning and are the heart of deep learning algorithms, also known as

artificial neural networks(ANNs) or simulated neural networks (SNNs). Their name and structure are inspired by the human brain, imitating the working strategy of the brain using mathematical methods to match the biological neuron [36].

Neurons are the simplest processing element of an ANN. ANNs consist of node layers, including an input layer, one or more hidden layers, and an output layer, as shown in Figure 6.1 [36]. Each node is linked to another and has several elements such as weight, activation function, and threshold. The nodes represent computational units and need inputs that should be processed in neurons to present the output. Weights are multiplied with inputs and then added in the summing function, then the sum is processed in the activation function. The output is then passed via an activation function to determine the output. If the output exceeds a threshold, the node is activated, and the data is passed into the next network layer. This results in the output of one node, which becomes the input of the next node. This data transmission procedure from one level to the next characterizes this neural network as a feedback network. The output is generated as shown in Figure 6.2 and the equations (6.10) and (6.11) [37].

Depending on the nature of the NN's system, the hidden network layers can be set in numerous ways. When weights are generally calibrated on the branched hidden layers, a relatively sophisticated approach called backpropagation was considered.

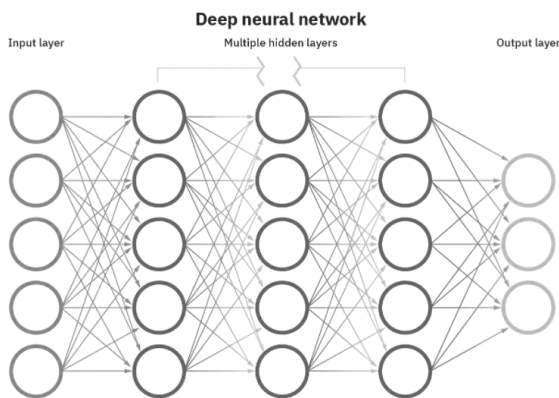


Fig - 6.1 Neural Network Architecture.

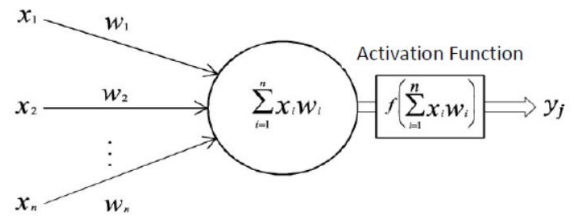


Fig - 6.2 Neuron Mathematical Function.

$$y_j = x_1 \cdot w_1 + x_2 \cdot w_2 + x_3 \cdot w_3 + x_n \cdot w_n \quad (6.10)$$

$$y_j = \sum_{i=1}^n x_i \cdot w_i \quad (6.11)$$

There are a few different forms of learning/training based on operation or system in which the neural network, the most generally used and known learning approach, is applied [37].

- Supervised Learning: the NN is fed with labeled datasets to find the correct decision at the test stage; the more this training/learning process, the more the accuracy [37].
- Unsupervised Learning: the NN is fed with unlabeled datasets (containing only the input data). The ANN will be able to categorize the data by clustering the data according to the distances and finding the patterns [37].
- Reinforcement Learning: it is a kind of Learning that involves the surrounding environment, starting by getting a state, taking action to change the state, and sending that action to either get a penalty or reward, to learn from its experience and reach the goal [37].

The steps of how the Neural Network works is shown in the following flowchart in Figure 6.3.

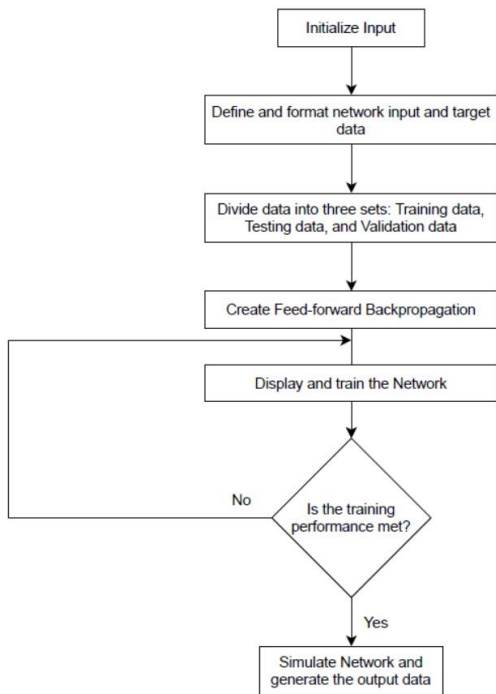


Fig - 6.3 FlowChart of Neural Network method.

6.2. Neural Network Training Algorithms

6.2.1. Feed-Forward Propagation

The input data is forwarded throughout the network in the feed-forward network. Every hidden layer accepts, processes, and passes the input data in accordance with the activation function. In other words, the information moves only in one direction – forward- from the input nodes, through the hidden nodes and to the output nodes, there are no cycles or loops in the network. The feed-forward network helps in forward propagation.

The processing takes place in two steps at each neuron in the hidden or output layer:

- Preactivation: it is a weighted sum of inputs. Based on this aggregated sum and activation function, the neuron decides whether to pass this information or not.
- Activation: the calculated weighted sum of inputs passed to the activation function. The activation function is a mathematical function which adds non-linearity to the network. There are four commonly used and popular activation functions – sigmoid, hyperbolic tangent (tanh), ReLU, and Softmax.

6.2.2. Backpropagation

The backpropagation is an efficient algorithm for training feedforward neural networks; it computes the gradient of the loss function concerning each weight by the chain rule, one layer at a time. Then, it iterates backward from that last layer and adjusts the weights between the input and the neuron to reduce the cost function and minimize the loss, as shown in Figure 6.4 [38].

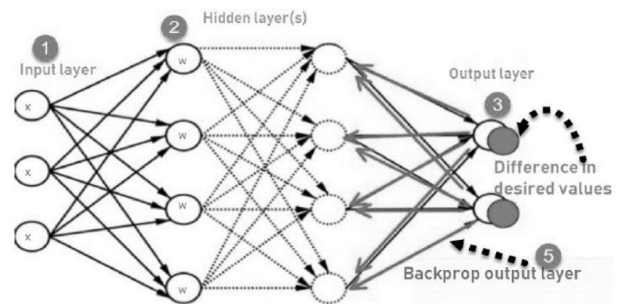


Fig - 6.4 Backpropagation.

6.2.3. Gradient Descent

The Gradient Descent is an algorithm for finding a local minimum of a differentiable function. It is used in machine learning to find the values of a function’s parameters/coefficients that minimize a cost function. The idea of this algorithm is to take repeated steps in the opposite direction of the gradient of a function at the current point (direction of the steepest descent). While if the steps were taken proportional to the positive of the gradient, the local maximum of a function would be approached, this is so-called Gradient Ascent as shown in Figure 6.5 [39].

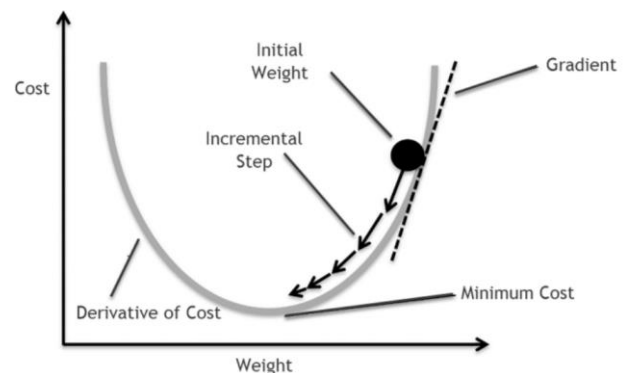


Fig - 6.5 Gradient Descent.

To perform the training phase in MATLAB for the optimal power flow problem, the learning algorithm used was the

Levenberg-Marquardt (LM) backpropagation. The Levenberg-Marquardt algorithm is designed to work specifically with loss functions which take the form of a sum of squared errors. It works without computing the exact Hessian matrix. Instead, it works with the gradient vector and the Jacobian matrix.

Levenberg-Marquardt is a combination of two other methods: The Gradient Descent and Gauss-Newton. Both methods are iterative algorithms, which means they use a series of calculations to find a solution. The gradient descent differs in that at each iteration, the solution updates by choosing values that make the function value smaller. In other words, the sum of the squared errors is reduced by moving toward the direction of steepest descent. Whereas, the Gauss-Newton is more accurate and faster than the gradient descent when close to the minimum error [40].

6.3. Power Flow Results using Neural Network method

To get the power flow results for the Networked Microgrids when the storage is either operating as a load or as a source using Neural Network, the tool which is used in MATLAB is the 'nntool' which opens the Network/Data manager window, which allows for importing, creating, using, and exporting Neural Networks and data.

6.3.1. Using Storage as a Load:

The custom neural network when the batteries are charging during the day is shown in Figure 6.6, Input (P) which is the input matrix that represents power demands and generation from the bus data as shown in Table 6.1.

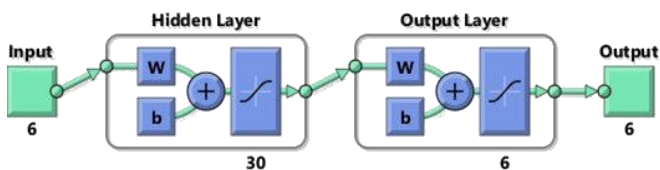


Fig - 6.6 Custom Neural Network – Storage as Load.

Table - 6.1 Input Matrix - Storage as Load.

Voltage Mag.	Angle Deg.	Load		Generation	
		MW	Mvar	MW	Mvar
1.000	0.000	0.000	0.000	15.000	0.000
1.000	0.000	4.125	0.336	2.000	0.000
1.000	0.000	5.729	1.023	2.400	0.000
1.000	0.000	4.050	0.555	2.000	0.000
1.000	0.000	1.257	0.310	0.000	0.000
1.000	0.000	1.056	0.240	0.000	0.000
1.000	0.000	0.600	0.100	6.000	0.000
1.000	0.000	2.850	0.487	1.600	0.000
1.000	0.000	2.803	0.410	1.600	0.000
1.000	0.000	3.766	0.443	2.400	0.000
1.000	0.000	0.764	0.036	0.000	0.000
1.000	0.000	0.503	0.021	0.800	0.000
1.000	0.000	0.345	0.011	0.000	0.000
1.000	0.000	0.629	0.008	0.000	0.000
1.000	0.000	0.642	0.012	0.500	0.000
1.000	0.000	0.580	0.150	6.000	0.000
1.000	0.000	0.650	0.085	0.000	0.000
1.000	0.000	2.673	0.096	2.000	0.000
1.000	0.000	0.839	0.135	0.400	0.000
1.000	0.000	1.400	0.128	0.800	0.000
1.000	0.000	1.360	0.112	0.800	0.000
1.000	0.000	1.651	0.145	0.800	0.000
1.000	0.000	0.420	0.025	0.000	0.000
1.000	0.000	0.500	0.045	0.000	0.000
1.000	0.000	0.637	0.033	0.000	0.000
1.000	0.000	0.788	0.095	0.000	0.000
1.000	0.000	0.125	0.050	0.000	0.000
1.000	0.000	0.169	0.020	0.000	0.000
1.000	0.000	0.200	0.043	0.500	0.000
1.000	0.000	1.050	0.032	0.800	0.000
1.000	0.000	0.213	0.012	0.000	0.000
1.000	0.000	0.133	0.025	1.200	0.000
1.000	0.000	0.200	0.038	0.000	0.000
1.000	0.000	0.426	0.080	4.000	0.000
1.000	0.000	0.318	0.078	0.000	0.000
1.000	0.000	0.356	0.081	0.000	0.000
1.000	0.000	0.459	0.088	0.000	0.000
1.000	0.000	2.420	0.091	1.600	0.000
1.000	0.000	4.900	0.635	2.400	0.000
1.000	0.000	2.416	0.060	1.600	0.000

Target (T) represents the desired output resulted from Newton-Raphson method shown in Table 5.1.

Using Feed forward backpropagation network, and the learning was performed according to the Levenberg-Marquardt algorithm (trainlm).

The simulation gives the following results:

Network Regression

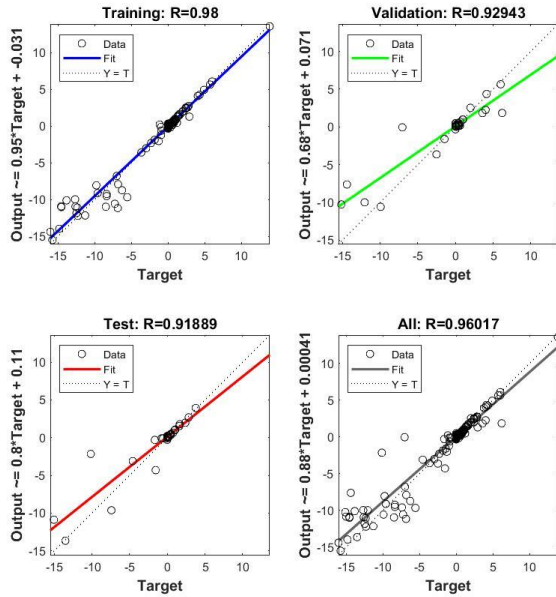


Fig - 6.7 Training, Validation, and Test Regression - Storage as Load.

The Network Regression figure displays the output of the network versus the target sets for training, validation and testing. To have the best results, the regression line should be fit at 45 degrees where all the outputs are equal to the targets. As shown in Figure 6.7, the R value equal to 0.96017, so the fit is extremely good as the value is close to '1' where it is 100% precise.

Neural Network Training Performance

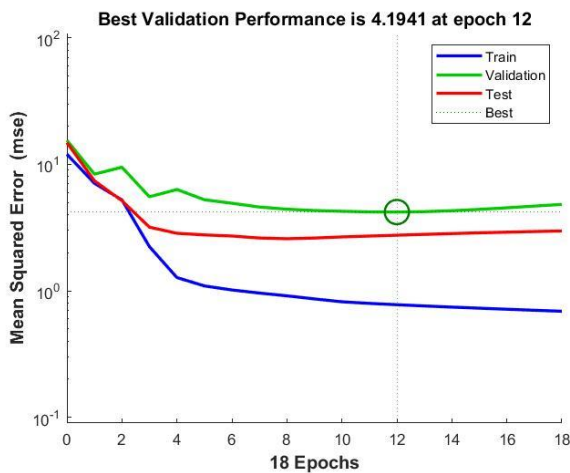


Fig - 6.8 Training Performance - Storage as Load.

The performance is calculated using the mean squared error. It minimizes the sum of squared errors between the network output and the targets according to epochs. The MSE is measured on the training, validation and testing sets.

Neural Network Training State

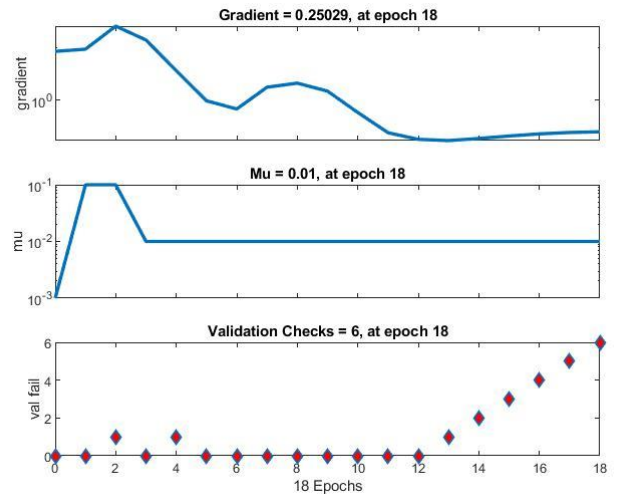


Fig - 6.9 Training State - Storage as Load.

The Training state represents the current progress/status of the training at a specific time while training is in progress.

Output (Y)

The output matrix of the neural network method:

Table - 6.2 Power Flow Results using Neural Network – Storage as Load.

Bus No.	Voltage		Load		Generation	
	Mag.	Angle Deg.	MW	Mvar	MW	Mvar
1	0.9858	-0.1886	0.1030	0.0722	13.5927	-3.0245
2	0.9859	-1.6073	4.3581	0.4504	2.5360	-0.0523
3	0.9806	-1.8750	5.6576	0.9660	2.3955	4.2582
4	0.9785	-2.3169	4.0955	0.5873	2.0179	1.4168
5	0.9846	-2.0335	1.2375	0.2213	0.1468	0.2413
6	0.9853	-4.2979	1.0783	0.1644	0.1415	-0.0267
7	0.9708	-3.6440	0.1662	0.0135	5.6461	1.8435
8	0.9808	-3.1096	2.6910	0.3831	1.5354	-0.3074
9	0.9839	-6.8049	2.7535	0.3076	1.5149	-1.2200
10	0.9817	-2.1566	3.9319	0.4621	1.9786	-0.0881
11	0.9816	-9.1327	0.8068	0.0753	0.3354	0.0926
12	0.9816	-9.6871	0.3513	0.0499	0.4705	0.8720
13	0.9858	-10.5819	0.3939	0.0545	0.2533	0.3314
14	0.9828	-10.0002	0.6583	0.0663	0.3382	0.4934
15	0.9810	-9.9858	0.5342	0.0582	0.4527	0.8061
16	0.9681	-3.5928	0.1499	0.0176	6.0692	0.9833
17	0.9840	-8.7449	0.6719	0.0835	0.2165	-0.3206
18	0.9852	-9.5356	2.5584	0.2080	1.9494	-0.6293
19	0.9827	-8.0721	0.7627	0.0945	0.2418	-0.1095
20	0.9774	-12.1792	1.4015	0.0728	0.5594	-0.1504
21	0.9767	-12.2331	1.3422	0.0708	0.5871	-0.1144
22	0.9783	-13.6664	1.7753	0.0713	0.6568	-0.0974
23	0.9850	-10.1224	0.4522	0.0600	0.2517	0.1501
24	0.9844	-9.6240	0.5218	0.0675	0.2415	-0.0668
25	0.9828	-9.2620	0.6635	0.0704	0.2991	0.0978
26	0.9832	-7.9221	0.8306	0.0899	0.2359	-0.3456
27	0.9884	-11.1737	0.2597	0.0543	0.1719	-0.0989
28	0.9877	-10.9879	0.2820	0.0492	0.2091	0.1566
29	0.9864	-10.5942	0.2302	0.0470	0.2673	0.2407
30	0.9765	-11.8424	0.9102	0.0645	0.6521	0.6589
31	0.9872	-10.9634	0.3064	0.0495	0.2254	0.2714
32	0.9850	-11.1004	0.1544	0.0327	0.4583	0.6949
33	0.9875	-10.9334	0.2977	0.0540	0.1935	-0.0231
34	0.9738	-7.6289	0.1245	0.0180	2.2527	1.8314
35	0.9871	-11.0323	0.3688	0.0697	0.1650	-0.2588
36	0.9868	-10.8727	0.3959	0.0722	0.1668	-0.2764
37	0.9860	-10.2761	0.4794	0.0783	0.1742	-0.3153
38	0.9822	-13.9883	2.5025	0.1230	1.6677	0.1972
39	0.9854	-15.5244	4.9251	0.6079	2.4151	2.4414
40	0.9828	-14.4144	2.5165	0.1354	1.6680	1.2862
Total			53.7001	6.2939	55.3509	11.8400

- Number of iterations: 18 iterations
- Execution time: Less than one second
- Total Losses: 1.6508 MW/5.5460 Mvar

6.3.2. Using Storage as a Source:

The custom neural network when the batteries are discharging during the night is shown in Figure 6.10, Input (P) which is the input matrix that represents power

demands and generation from the bus data as shown in Table 6.3.

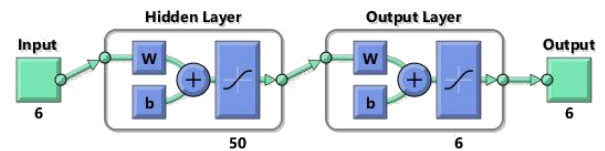


Fig - 6.10 Custom Neural Network – Storage as Source.

Table - 6.3 Input Matrix - Storage as Source.

Voltage Mag.	Angle Deg.	Load		Generation	
		MW	Mvar	MW	Mvar
1.000	0.000	0.000	0.000	15.000	0.000
1.000	0.000	2.125	0.336	1.600	0.000
1.000	0.000	3.329	1.023	1.920	0.000
1.000	0.000	2.050	0.555	1.600	0.000
1.000	0.000	1.257	0.310	0.000	0.000
1.000	0.000	1.056	0.240	0.000	0.000
1.000	0.000	0.600	0.100	6.000	0.000
1.000	0.000	1.250	0.487	1.280	0.000
1.000	0.000	1.203	0.410	1.280	0.000
1.000	0.000	1.366	0.443	1.920	0.000
1.000	0.000	0.764	0.036	0.000	0.000
1.000	0.000	0.503	0.021	0.800	0.000
1.000	0.000	0.345	0.011	0.000	0.000
1.000	0.000	0.629	0.008	0.000	0.000
1.000	0.000	0.642	0.012	0.500	0.000
1.000	0.000	0.580	0.150	6.000	0.000
1.000	0.000	0.650	0.085	0.000	0.000
1.000	0.000	0.673	0.096	1.600	0.000
1.000	0.000	0.439	0.135	0.320	0.000
1.000	0.000	0.600	0.128	0.640	0.000
1.000	0.000	0.560	0.112	0.640	0.000
1.000	0.000	0.851	0.145	0.640	0.000
1.000	0.000	0.420	0.025	0.000	0.000
1.000	0.000	0.500	0.045	0.000	0.000
1.000	0.000	0.637	0.033	0.000	0.000
1.000	0.000	0.788	0.095	0.000	0.000
1.000	0.000	0.125	0.050	0.000	0.000
1.000	0.000	0.169	0.020	0.000	0.000
1.000	0.000	0.200	0.043	0.500	0.000
1.000	0.000	0.250	0.032	0.640	0.000
1.000	0.000	0.213	0.012	0.000	0.000
1.000	0.000	0.133	0.025	1.200	0.000
1.000	0.000	0.200	0.038	0.000	0.000
1.000	0.000	0.426	0.080	4.000	0.000
1.000	0.000	0.318	0.078	0.000	0.000
1.000	0.000	0.356	0.081	0.000	0.000
1.000	0.000	0.459	0.088	0.000	0.000
1.000	0.000	0.820	0.091	1.280	0.000
1.000	0.000	2.500	0.635	1.920	0.000
1.000	0.000	0.816	0.060	1.280	0.000

Target (T) represents the desired output resulted from Newton-Raphson method shown in Table 5.2.

Using Feed forward backpropagation network, and the learning was performed according to the Levenberg-Marquardt algorithm (trainlm).

The simulation gives the following results:

Network Regression

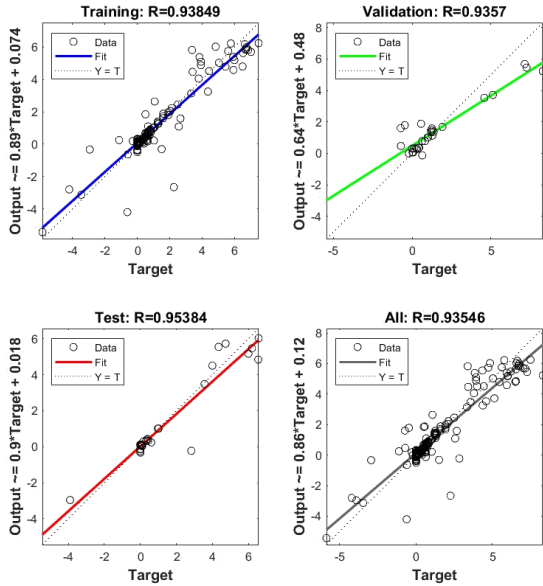


Fig - 6.11 Training, Validation, and Test Regression - Storage as Source.

As shown in Figure 6.11, the R value equal to 0.93546, so the fit is extremely good as the value is close to '1' where it is 100% precise.

Neural Network Training Performance

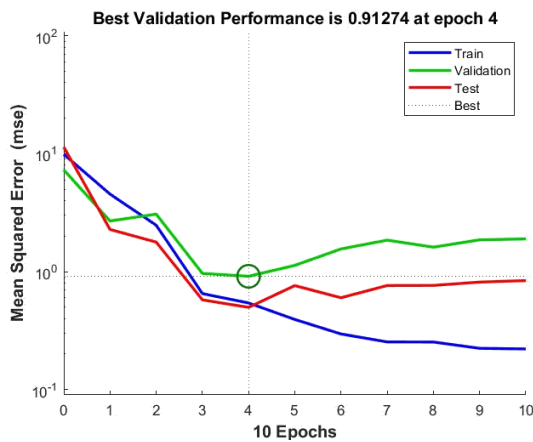


Fig - 6.12 Training Performance - Storage as Source.

The performance is also calculated using the mean squared error. It minimizes the sum of squared errors between the network output and the targets according to epochs. The

MSE is measured on the training, validation and testing sets.

Neural Network Training State

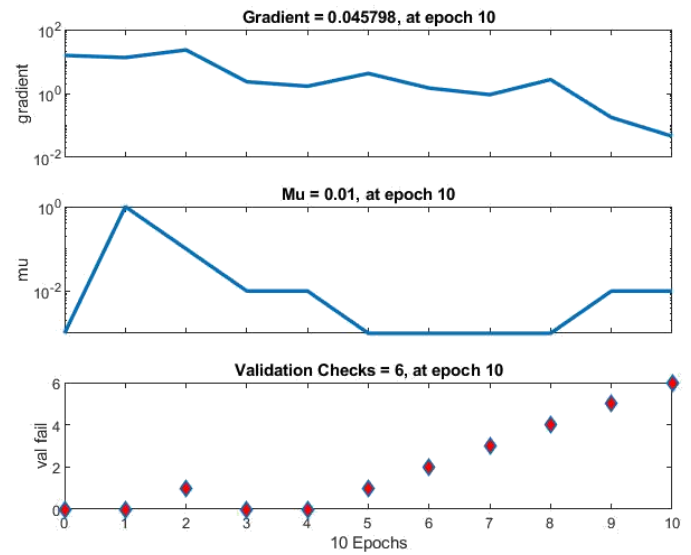


Fig - 6.13 Training State - Storage as Source.

Output (Y)

The output matrix of the neural network method:

Table - 6.4 Power Flow Results using Neural Network – Storage as Source.

Bus No.	Voltage	Angle	Load		Generation	
	Mag.	Deg.	MW	Mvar	MW	Mvar
1	1.0092	0.2838	0.02977	0.0262	-5.8046	-4.1702
2	0.97238	1.265	2.425	0.38396	1.5628	6.3557
3	0.97189	1.0938	3.3181	0.99196	1.8413	-0.56262
4	0.97729	2.6381	2.0767	0.51679	1.0866	5.9044
5	0.98658	1.88	1.4252	0.40696	0.03983	0.38936
6	0.98901	1.844	1.1758	0.32921	-0.17592	-0.14076
7	0.99074	3.4858	1.0247	0.08028	5.682	-1.8862
8	0.98442	3.2515	1.1717	0.42499	1.5694	-0.18368
9	0.99117	3.525	1.1826	0.38909	1.3492	0.34752
10	0.98483	3.7172	1.4808	0.38293	1.9573	-0.5673
11	0.98092	4.5107	0.71925	0.07099	0.11056	0.20475
12	0.98595	5.3936	0.48716	0.05353	0.67926	1.53E-01
13	0.98851	5.549	0.37749	0.04492	0.05979	-0.01387
14	0.98227	4.7898	0.59489	0.05639	-0.00274	0.069046
15	0.98201	5.0284	0.63701	0.05988	0.34453	0.25935
16	0.99509	4.0529	0.91689	0.11608	5.7863	-3.463
17	0.98717	5.0966	0.55391	0.07118	0.1824	-0.64944
18	0.98795	6.0261	0.67516	0.09174	1.4917	0.030751
19	0.99718	6.222	0.43683	0.07833	0.27891	-0.9201
20	0.99298	5.8749	0.51939	0.09033	0.69162	-0.94188
21	0.99261	5.8784	0.47999	0.07639	0.74422	-0.73821
22	0.98581	4.8025	0.81295	0.15776	0.73723	-0.3179
23	0.98811	5.4695	0.41129	0.04709	0.11427	-0.01091
24	0.98794	5.3808	0.44958	0.05155	0.17118	-0.18172
25	0.98366	4.8788	0.56878	0.05846	0.12703	-0.11577
26	0.98372	4.4673	0.70157	0.09489	0.1762	-0.37513
27	0.99493	5.82	0.2601	0.04495	0.12827	0.20652
28	0.99248	5.7303	0.28316	0.04311	0.06701	-0.04509
29	0.99401	5.7515	0.27064	0.04661	0.62316	0.21691
30	0.99249	5.6776	0.29571	0.04705	0.72359	0.17201
31	0.99116	5.6994	0.30772	0.0432	0.04851	-0.07655
32	0.99368	5.2246	0.20477	0.05228	1.3737	0.27519
33	0.99342	5.8418	0.29412	0.04386	0.10715	0.15153
34	0.99448	4.8439	0.4688	0.07508	4.2868	2.7764
35	0.9947	6.0262	0.35272	0.05084	0.13576	0.055875
36	0.99431	5.9946	0.37131	0.05248	0.1382	-0.08139
37	0.99278	5.8157	0.42556	0.05828	0.14491	-0.47658
38	0.98211	5.6262	0.90928	0.1141	1.2605	0.48675
39	0.98163	6.2446	2.4745	0.66272	1.8831	6.5345
40	0.9802	5.4537	0.9934	0.09916	1.0581	0.93375

Total 32.5643 6.58558 32.7791 9.604568

- Number of iterations: 10 iterations
- Execution time: Less than one second
- Total Losses: 0.214 MW/3.018 Mvar.

7. Discussion and Conclusion

7.1. Discussion

Power flow or load-flow studies are essential for planning the future expansion of power systems and determining the best operation of existing systems. The principal information obtained from the power flow study is the magnitude and phase angle of the voltage at each bus and the real and reactive power flowing in each line. Therefore, it is essential for the reliable and efficient operation of electrical networks. In this paper, optimal power flow is obtained for a networked microgrids system involving loads, decentralized sources of renewable energy (Solar PV panels and Wind turbines) and batteries as storage unit, using a conventional method (Newton Raphson method) and compared to a modern method (Neural Network method or Artificial Neural Network (ANN)). According to the results obtained above from MATLAB optimization and deep learning toolbox. The efficiency of the two methods is shown in Table 7.1 and Table 7.2.

In the first case where the batteries are operating as load, the losses efficiency are described in Table 7.1:

Table - 7.1 Comparison between NR and NN methods - Storage as Load.

Optimization Method	Losses and Efficiency
<i>Newton-Raphson method</i>	2.065 MW - 96% efficiency
<i>Neural Network method</i>	1.6508 MW - 97% efficiency

In the second case where the batteries are operating as source, the losses and efficiency are illustrated in Table 7.2:

Table - 7.2 Comparison between NR and NN methods - Storage as Source.

Optimization Method	Losses and Efficiency
<i>Newton-Raphson method</i>	0.896 MW - 97.1% efficiency
<i>Neural Network method</i>	0.214 MW - 99.3% efficiency

It is clearly shown that losses when the Neural Network was applied are lower and could produce more efficient results than the Newton-Raphson method. Also, the execution time is less when the OPF is performed using the Neural Network method, even though the iterations are more. For the Newton-Raphson method, the execution time takes more than one second in both cases. Still, Neural Network, a rapid convergence method, takes less than a second to convergence. The regression value is 0.93-0.98, approximately equal to 1, indicating that the results are good and have high accuracy and precision. According to the results obtained from both methods, it is clearly shown that the Neural Network method gave more accurate results and achieved the balance between load and generation to minimize the losses as much as possible. In other words, the generated active power from each bus was more accurate, and it was sufficient to supply the load with minimum losses. Furthermore, both methods did almost the same in producing other values, such as the bus voltages and angles.

7.2. Conclusions

This research focuses on studying the optimal power flow using a conventional method (Newton-Raphson) and AI method (Neural Network) for a networked MG test system. The load flow analysis considered two cases, when the storage units are charging from the generation sources during the day and when the storage units are supplying power at night to compensate the power when the PV panels can't generate power. Both methods were performed using Optimization and Deep Learning toolboxes in MATLAB. The Neural Network method based on AI represents more efficient results with minimum losses compared to the conventional method.

In future work, there are various technologies to be added to the microgrids architecture such as multiple energy storage systems (flywheels, electrolyzer-fuel cell), different energy rates related to the cost of the grid power depending on the target load (storage charge or consumer feeding), integrating the EVs to the microgrids which can help in global warming concerns and other grid services such as peak shaving and load shifting to increase the reliability of the system. The networked MG can also be used to validate other studies in the extended work, including reliability and resiliency analysis, economic dispatch, control and stability studies, and protection analysis.

REFERENCES

- [1] R. Morello, C. De Capua, G. Fulco and S. C. Mukhopadhyay, "A Smart Power Meter to Monitor Energy Flow in Smart Grids: The Role of Advanced Sensing and IoT in the Electric Grid of the Future," in *IEEE Sensors Journal*, vol. 17, no. 23, pp. 7828-7837, 1 Dec.1, 2017, doi: 10.1109/JSEN.2017.2760014.
- [2] B. Hanna and A. El-Shahat, "Optimal power flow for microgrids," 2017 IEEE Global Humanitarian Technology Conference (GHTC), 2017, pp. 1-3, doi: 10.1109/GHTC.2017.8239313.
- [3] R. Rigo-Mariani, B. Sareni, X. Roboam, and C. Turpin. "Optimal power dispatching strategies in smart-microgrids with storage." *Renewable and Sustainable Energy Reviews*, Elsevier, 2014, vol. 40, pp. 649-658. 10.1016/j.rser.2014.07.138. hal-01064368
- [4] H. Abdia, S. D. Beigvanda, and M. L. Scala, "A review of optimal power flow studies applied to smart grids and microgrids, *Renewable and Sustainable Energy Reviews*", Volume 71, 2017, Pages 742-766, ISSN 1364-0321, doi.org/10.1016/j.rser.2016.12.102.
- [5] S. Lin, J. Chen, "Distributed optimal power flow for smart grid transmission system with renewable energy sources", Volume 56, 2013, Pages 184-192, ISSN 0360-5442, <https://doi.org/10.1016/j.energy.2013.04.011>.
- [6] O. Amanifar and M. E. Hamedani Golshan, "Optimal Distributed Generation Placement and Sizing for Loss and THD Reduction and Voltage Profile Improvement," *Technical and Physical Problems of Engineering (IJTPE)*, vol. 3, no. 2, 2011.
- [7] F. R. Pazheri, M. F. Othman, N. H. Malik, and S. O. K, "Economic and Environmental Dispatch at Highly Potential Renewable Area with Renewable Storage," *International Journal of Environmental Science and Development*, pp. 177-182, 2012.
- [8] Y. M. Atwa, E. F. El-Saadany, M. M. A. Salama, and R. Seethapathy, "Optimal renewable resources mix for distribution system energy loss minimization," *IEEE Transactions on Power Systems*, vol. 25, no. 1, pp. 360-370, 2010.
- [9] S. Sichilalu, T. Mathaba, and X. Xia, "Optimal control of a wind-PV-hybrid powered heat pump water heater," *Applied Energy*, vol. 185, pp. 1173-1184, 2017.

- [10] E. R. Sanseverino, M. L. Di Silvestre, M. G. Ippolito, A. De Paola, and G. Lo Re, "An execution, monitoring and replanning approach for optimal energy management in microgrids," *Energy*, vol. 36, no. 5, pp. 3429–3436, 2011
- [11] C. Chen, S. Duan, T. Cai, B. Liu, and G. Hu, "Smart energy management system for optimal microgrid economic operation," *IET Renewable Power Generation*, vol. 5, no. 3, pp. 258–267, 2011.
- [12] Y. Levron, J. M. Guerrero, and Y. Beck, "Optimal power flow in microgrids with energy storage," *IEEE Transactions on Power Systems*, vol. 28, no. 3, pp. 3226–3234, 2013.
- [13] A. Bracale, P. Caramia, G. Carpinelli, E. Mancini, and F. Mottola, "Optimal control strategy of a DC micro grid," *International Journal of Electrical Power & Energy Systems*, vol. 67, pp. 25–38, 2015.
- [14] E. Riva Sanseverino, N. Nguyen Quang, M. L. Di Silvestre, J. M. Guerrero, and C. Li, "Optimal power flow in three-phase islanded microgrids with inverter interfaced units," *Electric Power Systems Research*, vol. 123, pp. 48–56, 2015.
- [15] J. Shen, C. Jiang, Y. Liu, and X. Wang, "A Microgrid Energy Management System and Risk Management under an Electricity Market Environment," *IEEE Access*, vol. 4, pp. 2349–2356, 2016.
- [16] H. Hassanzadehfard, S. M. Moghaddas-Tafreshi, and S. M. Hakimi, "Optimization of grid-connected microgrid consisting of PV/FC/UC with considered frequency control," *Turkish Journal of Electrical Engineering & Computer Sciences*, vol. 23, no. 1, pp. 1–16, 2015.
- [17] R. Yu, W. Zhong, S. Xie, C. Yuen, S. Gjessing, and Y. Zhang, "Balancing Power Demand Through EV Mobility in Vehicle-to-Grid Mobile Energy Networks," *IEEE Transactions on Industrial Informatics*, vol. 12, no. 1, pp. 79–90, 2016.
- [18] F. Laureri, L. Puliga, M. Robba, F. Delfino, and G. Odena Bultò, "An optimization model for the integration of electric vehicles and smart grids Problem definition and experimental validation," in *Proceedings of the 2nd IEEE International Smart Cities Conference, ISC2 2016*, September 2016.
- [19] N. G. Paterakis, O. Erdinc, I. N. Pappi, A. G. Bakirtzis, and J. P. S. Catalao, "Coordinated Operation of a Neighborhood of Smart Households Comprising Electric Vehicles, Energy Storage and Distributed Generation," *IEEE Transactions on Smart Grid*, vol. 7, no. 6, pp. 2736–2747, 2016.
- [20] C.-H. Lin, W.-L. Hsieh, C.-S. Chen, C.-T. Hsu, and T.-T. Ku, "Optimization of photovoltaic penetration in distribution systems considering annual duration curve of solar irradiation," *IEEE Transactions on Power Systems*, vol. 27, no. 2, pp. 1090–1097, 2012.
- [21] M. Bianchi, L. Branchini, C. Ferrari, and F. Melino, "Optimal sizing of grid-independent hybrid photovoltaic-battery power systems for household sector," *Applied Energy*, vol. 136, pp. 805–816, 2014.
- [22] R. Nazir, K. Kanada, Syafii, and P. Coveria, "Optimization active and reactive power flow for PV connected to grid system using Newton Raphson method," in *Proceedings of the 2nd International Conference on Sustainable Energy Engineering and Application, ICSEEA 2014*, pp. 77–86, idn, October 2014.
- [23] M. GEORGIEV, R. Stanev and A. Krusteva, "Optimized power flow control of smart grids with electric vehicles and DER," *2019 16th Conference on Electrical Machines, Drives and Power Systems (ELMA)*, 2019, pp. 1-6, doi: 10.1109/ELMA.2019.8771575.
- [24] B. Kim, O. Lavrova, "Optimal power flow and energy-sharing among multi-agent smart buildings in the smart grid," *2013 IEEE Energytech*, 2013, pp. 1-5, doi: 10.1109/EnergyTech.2013.6645336.
- [25] D. Ke, C. Y. Chung, and Y. Sun, "A novel probabilistic optimal power flow model with uncertain wind power generation described by customized Gaussian mixture model," *IEEE Transactions on Sustainable Energy*, vol. 7, no. 1, pp. 200–212, 2016.
- [26] G. J. Sebastián, C. J. Alexander, and G. Mauricio, "Stochastic AC Optimal Power Flow Considering the Probabilistic Behavior of the Wind, Loads and Line Parameters," *Ingeniería, Investigación y Tecnología*, vol. 15, no. 4, pp. 529–538, 2014.
- [27] H. T. Jadhav and R. Roy, "Stochastic optimal power flow incorporating offshore wind farm and electric vehicles," *International Journal of Electrical Power & Energy Systems*, vol. 69, pp. 173–187, 2015.
- [28] S.-Y. Lin and A.-C. Lin, "RLOPF (risk-limiting optimal power flow) for systems with high penetration of wind power," *Energy*, vol. 71, pp. 49–61, 2014.

[29] D. Owerko, F. Gama and A. Ribeiro, "Optimal Power Flow Using Graph Neural Networks," ICASSP 2020 - 2020 IEEE International Conference on Acoustics, Speech and Signal Processing (ICASSP), 2020, pp. 5930-5934, doi: 10.1109/ICASSP40776.2020.9053140.

[30] H. kaur, Y. S. Brar and J. S. Randhawa, "Optimal power flow using power world simulator," 2010 IEEE Electrical Power & Energy Conference, 2010, pp. 1-6, doi: 10.1109/EPEC.2010.5697188.

[31] S.A. Soliman and A.H. Mantawy, Optimal Power Flow: Modern Optimization Techniques with Applications in Electric Power Systems, Energy Systems, DOI 10.1007/978-1-4614-1752-1_5, # Springer Science+Business Media, LLC 2012

[32] M. Ebeed, S. Kamel, and, F. Jurado, "Optimal Power Flow Using Recent Optimization Techniques" in Classical and Recent Aspects of Power System Optimization, 2018, pp. 157-183

[33] A. Ismail. Class Lecture. Topic:" Lecture 5 - OPTIMAL POWER FLOW.". College of Electrical Engineering, Rochester Institute of technology, Dubai, 2020.

[34] M. N. Alam, S. Chakrabarti and X. Liang, "A Benchmark Test System for Networked Microgrids," in IEEE Transactions on Industrial Informatics, vol. 16, no. 10, pp. 6217-6230, Oct. 2020, doi: 10.1109/TII.2020.2976893.

[35] H. Saadat, Power System Analysis. McGraw-Hill Book Company, New York, 1999.

[36] IBM Education, 2020. What are Neural Networks?. [online] ibm.com. Available at: <<https://www.ibm.com/cloud/learn/neural-networks>> [Accessed 22 October 2021].

[37] P. Kim, MATLAB Deep Learning with Machine Learning, Neural Networks and Artificial Intelligence. 2017.

[38] D. Johnson, 2021. Back Propagation Neural Network: What is Backpropagation Algorithm in Machine Learning?. [online] Guru99. Available at: <<https://www.guru99.com/backpropagation-neural-network.html>> [Accessed 24 October 2021].

[39] Analytics Vidhya. How Does the Gradient Descent Algorithm Work in Machine Learning?. 2020. [online] Available at: <[does-the-gradient-descent-algorithm-work-in-machine-learning/> \[Accessed 27 October 2021\].](https://www.analyticsvidhya.com/blog/2020/10/how-</p></div><div data-bbox=)

[40] Wikiwand. n.d. Levenberg–Marquardt algorithm | Wikiwand. [online] Available at: <https://www.wikiwand.com/en/Levenberg%E2%80%93Marquardt_algorithm> [Accessed 28 October 2021].